Science of the Total Environment 806 (2022) 150234

Contents lists available at ScienceDirect

Science of the Total Environment

journal homepage: www.elsevier.com/locate/scitotenv

Effect of diurnal temperature range on bioleaching of sulfide ore by an artificial microbial consortium

Xiaodi Fang[a], Shuiyu Sun[a,b], Xiaojian Liao[a], Shoupeng Li[a,*], Siyu Zhou[a], Qiaowei Gan[a], Liuting Zeng[a], Zhijie Guan[a]

[a] Guangzhou Key Laboratory Environmental Catalysis and Pollution Control, Guangdong Key Laboratory of Environmental Catalysis and Health Risk Control, School of Environmental Science and Engineering, Institute of Environmental Health and Pollution Control, Guangdong University of Technology, Guangzhou 510006, China
[b] Guangdong Polytechnic of Environmental Protection Engineering, Foshan 528216, China

HIGHLIGHTS

- The effect of diurnal temperature range (DTR) on ore dissolution was first studied.
- DTR induced inhibition of the bioleaching efficiency.
- DTR inhibits the initial secretion of extracellular polymeric substance (EPS).
- The increased EPS (from 3.91 mg/L to 15.30 mg/L, TOC) help reduce DTR inhibition.
- DTR had no obvious effect on the mineralogical characteristics.

GRAPHICAL ABSTRACT

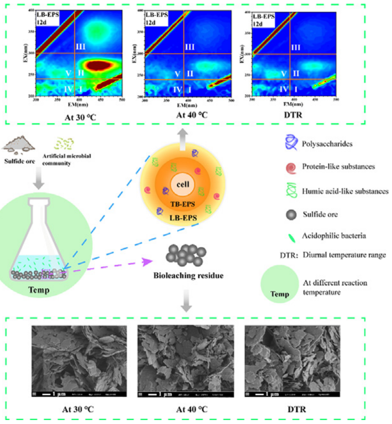

ARTICLE INFO

Article history:
Received 18 June 2021
Received in revised form 28 August 2021
Accepted 5 September 2021
Available online 9 September 2021

Editor: Huu Hao Ngo

Keywords:
Diurnal temperature range
Bioleaching
Sulfide ore
Artificial microbial consortium
Extracellular polymeric substances

ABSTRACT

Temperature is considered to be one of the main factors affecting bioleaching, but few studies have assessed the effects of diurnal temperature range (DTR) on the bioleaching process. This study investigates the effects of different bioleaching temperatures (30 and 40 °C) and DTR on the bioleaching of metal sulfide ores by microbial communities. The results showed that DTR had an obvious inhibitory effect on the bioleaching efficiency of the artificial microbial community, although this effect was mainly concentrated in the early and middle stages (0–18 days) of exposure, gradually decreasing until almost disappearing in the late stage (18–24 days). Extracellular polymeric substance (EPS) analysis showed that DTR did not change the composition of the EPS matrix (humic acid-like substances, polysaccharides and protein-like substances), but had a significant effect on the generative behavior of EPS, inhibiting the secretion of EPS during the early and middle stages of the bioleaching process. However, the continual increase in EPS secretion in the bioleaching system gradually reduced the adverse effects of DTR on mineral dissolution. X-ray diffraction (XRD), Fourier transform infrared (FTIR) and Scanning electron microscopy- energy dispersive spectrometry (SEM-EDS) analysis of the bioleached residue showed that DTR had no obvious effect on the mineralogical characteristics of sulfide ore. Therefore, in industrial sulfide ore bioleaching applications, in order to accelerate the artificial microbial community start-up process, temperature control measures should be increased in the bioleaching process to reduce the adverse effects of DTR on mineral dissolution.

---

* Corresponding author.
E-mail address: lsp@gdut.edu.cn (S. Li).

https://doi.org/10.1016/j.scitotenv.2021.150234

1. Introduction

Bioleaching technology refers to the use of acidophilic microbial oxidation to convert metals contained in minerals, such as sulfide ore, into free metal ions (Brierley and Brierley, 2001). Due to its low operational costs, mild reaction conditions and low environmental impact, this process has been widely used for metal recovery from sulfide ores in recent years (Muravyov and Panyushkina, 2020). However, the low efficiency of bioleaching technology has limited its widespread development and application (J.F. Li et al., 2021; Li et al., 2013). Many efforts have been made in recent decades to increase the efficiency of bioleaching processes, with the use of artificial microbial consortia achieving good results in laboratory level studies (Liao et al., 2019; Ma et al., 2019). The typical bioleaching microorganisms, including *Leptospirillum ferrooxidans*, *Acidithiobacillus ferrooxidans*, *Acidithiobacillus thiooxidans*, *Ferroplasma acidiphilum*, *Sulfobacillus thermosulfidooxidans* and *Acidithiobacillus caldus*, were widespread in bioleaching systems (Brierley, 2008; Panda et al., 2015). A high-efficient bioleaching system was generally performed by artificial microbial consortia constructed in a collaborative way (Liao et al., 2019). Therefore, the six above bioleaching microorganisms were selected to construct an artificial microbial consortia based on the characteristics of sulfide ore and the types of bioleaching microorganisms, which achieved high bioleaching efficiency for the target minerals.

However, temperature is a key factor affecting bioleaching efficiency, with varying temperatures having a significant impact on the microbial behavior and bioleaching effect (Boxall et al., 2017; Yu et al., 2019). Under natural conditions a large difference exists between day-time and night-time temperatures, with the global daily average temperature difference being more than 10 °C (Zhuang and Zhang, 2020). Therefore, effect of diurnal temperature range (DTR) on bioleaching efficiency is an important aspect that must be accounted for in the industrial application of bioleaching systems developed under laboratory conditions (J.F. Li et al., 2021). Most previous studies have been carried out under constant temperature conditions (Camacho et al., 2020; Ye et al., 2017), with few studies investigating the effect of DTR on microbial behavior and mineral dissolution during bioleaching. Therefore, in the present study, DTR was simulated to explore its impact on the bioleaching process.

Pyrite is the most widely distributed natural metal sulfide ore and pyrite oxidation is one of the key reactions in the bio-oxidation of bare metal sulfide deposits, especially in low-grade metal sulfide ore bioleaching (Banerjee et al., 2017; Sethurajan et al., 2018; Tabelin et al., 2020). Therefore, high pyrite sulfide ore (HPSO) was selected as the research object in this study, to establish the influence of DTR on bioleaching. During the bioleaching process, sulfide minerals are dissolved continuously due to the action of bacteria. However, a passivation layer can be formed on the surface of minerals, which can consist of elemental sulfur, jarosite or secondary minerals, inhibiting sulfide mineral dissolution (Xia et al., 2018; Yang et al., 2015). In addition, previous studies have shown that an increase in temperature is conducive to the formation of jarosite (Jia et al., 2018; Yang et al., 2015). However, little is known about whether DTR affects the formation of a passivation layer and hence, the dissolution of minerals. Therefore, detailed analyses of the mineralogical characteristics and surface speciation of sulfide minerals under DTR conditions, help further our understanding of the effect of DTR on the bioleaching process, promoting the industrial application potential of this technology.

Bioleaching of sulfide ores involves interaction between the mineral phase, leachate phase and microbial phase. Extracellular polymeric substances (EPS) are high molecular weight polymer mixtures secreted in vitro by microorganisms to protect cells against harsh environmental conditions (Hu et al., 2020), playing an important role in almost all microbial interface activities (Tian, 2008). EPS is not only conducive to the adsorption of acidophils on mineral surfaces, but can also enrich Fe^{3+} in mineral ore via complexation, resulting in the continuous oxidation and dissolution of minerals (Bellenberg et al., 2019; Li and Sand, 2017). Bound EPS on the surface of minerals and bacteria, has been shown to have a major influence on bioleaching (Ye et al., 2021). The dynamic double-layer structure of bound EPS is composed of loosely bound EPS (LB-EPS) and tightly bound EPS (TB-EPS) (Liang et al., 2019; Ye et al., 2021). However, most previous studies have focused on EPS as a whole single component (Li and Sand, 2017; Yu et al., 2018), with few studies investigating the dynamic relationship between the two EPS layer types. In addition, the composition of EPS is dynamic, continually changing both physically and chemically under varying bioleaching conditions (Hu et al., 2020; Li and Sand, 2017). Temperature has a significant influence on the production and generative behavior of EPS (More et al., 2014; Premnath et al., 2021). Most previous studies have focused on EPS production under constant temperature conditions (Yu et al., 2019) and few reports have assessed the effect of DTR on EPS production during the metal sulfide bioleaching process. Therefore, establishing the influence of DTR on the dynamic change in LB-EPS and TB-EPS components and concentrations during the bioleaching process, is important for the effective industrial application of bioleaching technologies.

In conclusion, DTR is an important influencing factor in the process of promoting bioleaching from laboratory level to industrial application. However, the effect of DTR on bioleaching is still unclear at present, which needs further study and verification. Therefore, based on previous studies, the main objectives of this study were as follows: (1) to explore the effect of DTR on bioleaching of sulfide ore by an artificial microbial consortium; and (2) to reveal the mechanism by which DTR inducing inhibition of the bioleaching efficiency. Three-dimensional excitation emission matrix (3D-EEM) fluorescence spectroscopy, X-ray diffraction (XRD), Fourier transform infrared (FTIR) spectroscopy and Scanning electron microscopy-energy dispersive spectrometry (SEM-EDS) were used to determine the EPS components and the mineralogical characteristics, respectively, during bioleaching. Based on this analysis of the mechanism of microbial action on minerals, the effect of DTR on EPS generative behavior and mineral dissolution mechanisms were established, which had important guiding significance for the industrial application of bioleaching.

2. Materials and methods

2.1. Mineral samples

Mineral samples were obtained from Renhua county, Guangdong Province, China. All mineral samples were crushed and 85% of the mass was passed through a 200-mesh sieve to obtain powders with particle sizes of <74 μm. Mineralogical analysis of the mineral samples was performed by XRD, showing that the main components were pyrite, calcite and quartz (Fig. 1). The chemical composition of the minerals was analyzed by XRF, showing that the mineral was mainly composed of 33.96% Fe, 19.59% S, 17.96% Ca, 15.92% Si, 6.22% Al, 2.06% K, and 1.67% Mg, with a 2.62% content of other trace elements.

2.2. Microbial strains and culture conditions

Six typical microbial bioleaching strains, including *Leptospirillum ferrooxidans* DX-m, *Acidithiobacillus ferrooxidans* DX-m, *Acidithiobacillus thiooxidans* A01, *Ferroplasma acidiphilum* DSM 28986, *Sulfobacillus thermosulfidooxidans* DSM 9293T and *Acidithiobacillus caldus* DSM 8584T, were provided by the Key Lab of Bio-hydrometallurgy of the Ministry of Education (Central South University, China). The culture conditions for the six typical strains are listed in detail in Table S1 (Supplementary information). The culture medium was 9 K basal medium, containing 3.00 g/L $(NH_4)_2SO_4$, 0.10 g/L KCl, 0.50 g/L K_2HPO_4, 0.50 g/L $MgSO_4 \cdot 7H_2O$, and 0.01 g/L $Ca(NO_3)_2$ (Ma et al., 2019). When the bacterial cultures were in logarithmic phase they were centrifuged at 955 ×*g* for 5 min to remove the sediment and then at 10,619 ×*g* for

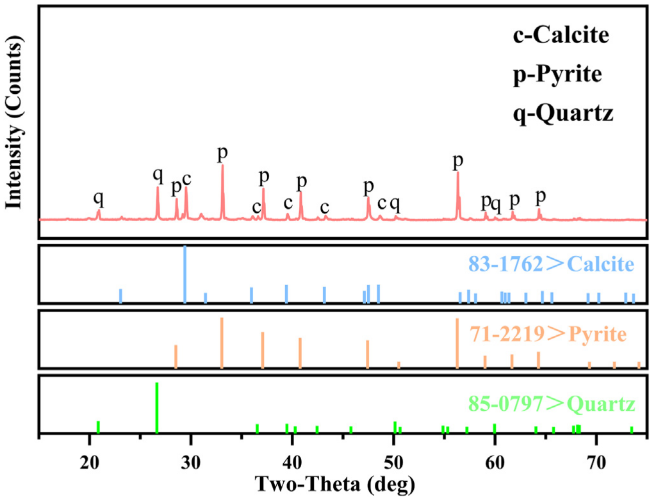

Fig. 1. The XRD spectra of the original mineral ore material.

20 min to obtain live cell pellets, which were resuspended in fresh 9 K basal medium for subsequent bioleaching experiments.

2.3. Bioleaching experiments

Bioleaching experiments were conducted in 250-mL flasks containing 100 mL of sterilized 9 K basal medium, with 5 g of mineral samples added and bioleached at 170 rpm for 24 days. Before the start of bioleaching experiments, sulfuric acid was used to adjust the pH of the medium to 1.8, with the adjustment repeated continually until the pH remained stable. The six typical bioleaching strains were inoculated into the culture medium at equal cell number ratios, resulting in a total inoculation concentration of 1×10^7 cells/L. To assess the effect of different bioleaching temperature conditions and to simulate DTR, three experimental groups were established, with bioleaching performed at a constant temperature of 30 °C (group A), 40 °C (group B), or with a DTR of 40 °C for 16 h and 30 °C for 8 h (group C). Sterile control groups were compared under each temperature condition without any inoculum addition. Sterile water and 9 K basic culture medium were added to supplement water evaporation and sampling loss during the bioleaching process, respectively.

2.4. EPS extraction and analysis

During the bioleaching process, the modified heat extraction method was used to extract bound EPS (including LB-EPS and TB-EPS) every 6 days (Liang et al., 2019; Yu et al., 2008). Detailed descriptions of the extraction process are provided in Text S1 (Supplementary information). 3D-EEM (F-4600, Hitachi, Japan) was used to scan the EPS samples from each group at different bioleaching times at a speed of 2400 nm/min, assessing excitation (Ex) wavelengths from 200 to 400 nm and emission (Em) wavelengths from 300 to 500 nm at 5 nm scan intervals. All samples were determined at pH 4.0 and 25 °C. In order to eliminate the Raman peak scattering influence of water, the fluorescence intensity of distilled water samples were used for background correction of the scan results.

Fluorescence regional integration (FRI) was used for the quantitative analysis of soluble organic matter in 3D-EEM fluorescence spectroscopy (Chen et al., 2003; Ye et al., 2021), with the specific FRI calculation method provided in Text S2 (Supplementary information).

2.5. Analytical techniques

During the bioleaching process, supernatant samples were collected every 48 h. The ORP and pH of extracts were determined using an ORP meter (STORP 1, OHAUS, US) with an Ag/AgCl reference electrode and a digital pH meter (STARTER 2100, OHAUS, US), respectively. The ferric ion [Fe^{3+}] and total iron [TFe] concentrations in the bioleaching solution were determined by 5-sulfosalicylic acid spectrophotometry (Karamanev et al., 2002). Each data point and error bar represents the mean value and standard deviation, respectively. Variance analysis was performed using IMB SPSS Statistics v.26.

The total organic carbon (TOC) concentration in EPS samples was measured using a TOC analyzer (Japan Shimadzu TOC-VCPH, Japan). The polysaccharide concentration in EPS samples was measured by the anthrone method (Liang et al., 2019). The detailed introduction of analytical techniques was provided in Table S2 (Supplementary information).

2.6. Mineralogical analysis

After the leaching experiment, mineral residue samples were collected, washed with ultrapure water and dried in a freeze dryer (LGJ-10C, Sihuan, China) for subsequent analysis. The phase change of minerals was analyzed by XRD (SmartLab 9 Kw, Rigaku, Japan) and changes in the surface functional groups of minerals were analyzed by FTIR spectroscopy (Nicolet 6700, Thermo-Fisher, US). The changes in surface characteristics of minerals were analyzed by SEM-EDS (Gemini 300, Zeiss, Germany).

3. Results and discussion

3.1. Bioleaching of sulfide ore under different temperature conditions

Fig. 2 shows the relationships among [TFe], [Fe^{3+}], pH and ORP in the process of bioleaching and acid leaching under different temperature conditions. Compared with the abiotic control groups, significant metal dissolution was observed in the bioleaching groups, indicating that the presence of microorganisms significantly promoted mineral oxidation. According to the changes in physical and chemical parameters, the bioleaching process can be divided into early (adaptation period, 0–6th day), middle (growth period, 6–18th day) and late (stable period, 18–24th day) stages.

In the early stage of bioleaching, the minerals in group A dissolved first, with the [TFe] increasing rapidly to 2.35 g/L, while the minerals in group B and group C treatments dissolved more slowly, with the [TFe] increasing to 1.20 g/L and 1.14 g/L, respectively (Fig. 1a). After 18 days of treatment, the [TFe] of group A and B increased sharply to 12.09 g/L and 12.23 g/L, respectively, while the [TFe] of group C only increased to 9.75 g/L. In the late stage, the [TFe] of group A and B increased slowly, while the [TFe] of group C continued to increase until it remained flat. According to variance analysis, there were no significant differences observed in [TFe] among the three bioleaching treatment groups after 24 days ($p > 0.05$), with final [TFe] of 13.09 g/L, 13.42 g/L and 13.57 g/L, respectively. In the early stage, the rapid increase in [TFe] in group A can be attributed to efficient microbial community adaptation to the extreme environment of the oligotrophic bioleaching system, after inoculation from the eutrophic cultivation system (Ma et al., 2019). In contrast, the increased temperature in group B and DTR conditions of group C were not conducive to rapid microbial community adaptation to the extreme environment. In the middle stage of bioleaching, the adverse effect of DTR on bioleaching system significantly increased, resulting in the slow dissolution of minerals. In the late stage, the adverse effect of DTR on mineral dissolution gradually decreased until almost disappeared and therefore, subjection to a DTR induced no significant effect on the final bioleaching results.

Fig. 2b shows the trend in [Fe^{3+}] in each treatment group. In the abiotic control groups, due to the absence of microbial oxidation, the rise of [Fe^{3+}] was slow, indicating that pyrite dissolution under acidic conditions is limited without microbial oxidation. When bacteria were present to oxidize and decompose minerals, the [Fe^{3+}] in the three bioleaching groups increased continuously, finally stabilizing in the late treatment stage. The

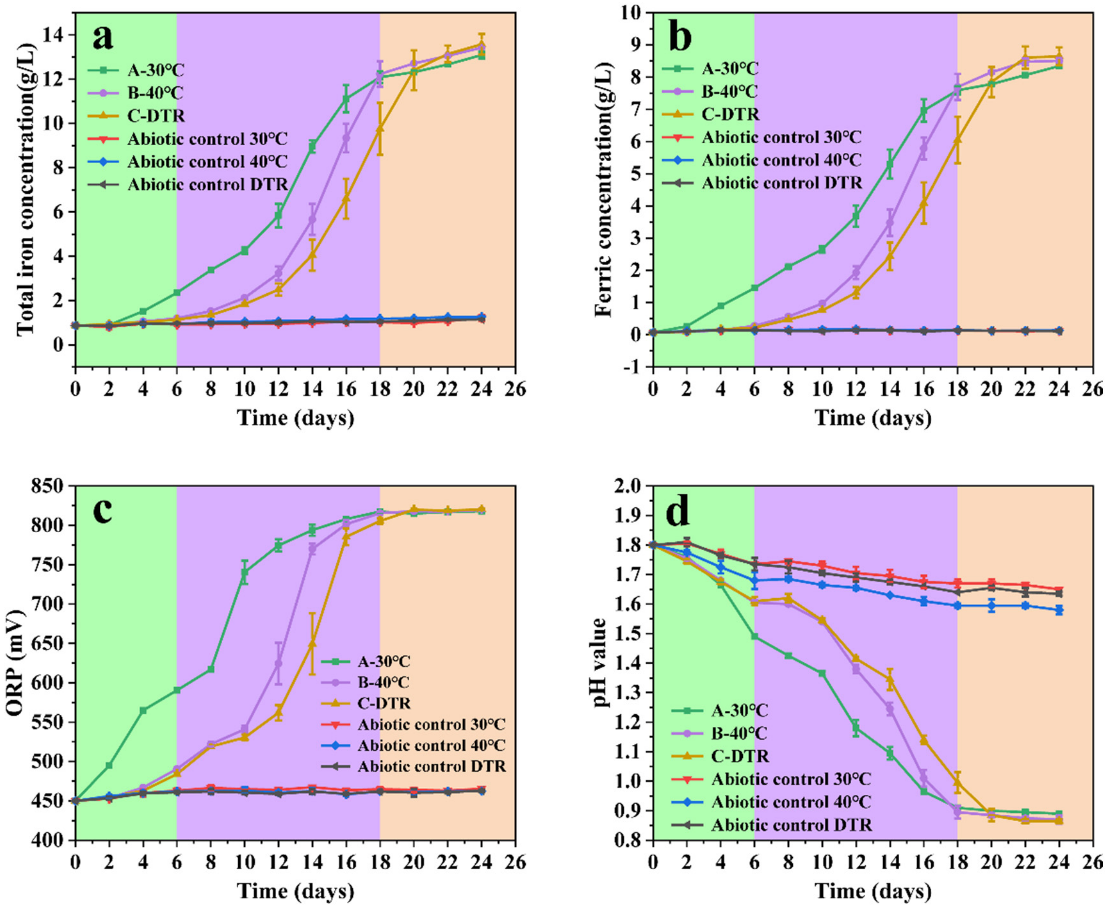

Fig. 2. Variation in physicochemical parameters during the 24 days bioleaching treatment. (a) Total iron concentration; (b) ferrous ion concentration; (c) ORP; (d) pH.

observed increase in ferric ion concentration was similar to the increasing trend of [TFe]. It is generally believed that ferric ion can be used as oxidant to promote the dissolution of pyrite (Eq. (1)) (Liao et al., 2019). Therefore, an increase in ferric ion is conducive to the continuous dissolution of minerals. In the first 6 days of treatment, the [Fe^{3+}] in group A, B and C increased to 1.45 g/L, 0.28 g/L and 0.22 g/L, respectively. In the first 18 days of treatment, the [Fe^{3+}] in group A and B increased sharply to 7.59 g/L and 7.69 g/L, respectively, while the [Fe^{3+}] in group C only increased 6.05 g/L. indicating that the DTR significantly inhibited the middle stage release of Fe^{3+}, resulting in a lower total iron dissolution rate. However, the [Fe^{3+}] of group C continued to increase and reached similar results with the other two bioleaching groups in the late stage of bioleaching.

$$FeS_2 + 2Fe^{3+} \rightarrow 3Fe^{2+} + 2S^0 \qquad (1)$$

ORP is a major parameter in the bioleaching process, playing a key role in mineral bio-oxidation efficiency (Liao et al., 2019). During the whole dissolution process, the ORP of sterile control systems remained below 470 mV. However, the ORP of all bioleaching treatment groups increased rapidly, becoming relatively stable in the late treatment stage (Fig. 2c). In the first 6 days, the ORP of group A increased most rapidly, reaching to 591 mV, while the ORP's of group B and C increased to 491 mV and 484 mV, respectively. The ORP is closely related to the ratio of [Fe^{3+}] to [Fe^{2+}] (Ma et al., 2019), with the higher ORP in group A being due to its higher ferric ion concentration (Fig. 2b). In addition, it has previously been reported that the biological oxidation of pyrite is slower when the ORP is lower than 540 mV (Blight et al., 2000). Therefore, the lower ORP's in group B and C in the early stage of treatment were not conducive to the dissolution of minerals. In the middle stage, the slowest rise in ORP in group C could be attributed to lowest microbial adaptation to the extreme environment under DTR conditions, indicating that the inhibition of DTR on mineral dissolution significantly increased. By the end of the experimental period, all three bioleaching groups exhibited similar ORP's, at around 820 mV.

A key index of sulfide ore oxidation is the pH of the bioleaching system. The pH of the abiotic groups decreased slowly, with the highest decrease in pH observed at 40 °C, indicating that an increase of temperature could promote the abiotic dissolution of minerals to some extent, although the effect was negligible compared with the equivalent bioleaching group. During the process of bioleaching the pH continually decreased, finally stabilizing at about 0.87 (Fig. 2d). The reason for this obvious decrease can be attributed to microbial promotion of the dissolution of pyrite from HPSO and the continual production of acid (Eq. (2)) (Igarashi et al., 2020). In the first 6 days of treatment, the pH of group A decreased fastest, from 1.8 to 1.49, while the pH of group B and C decreased to only 1.60 and 1.61, respectively. After 18 days of treatment, the pH of group A, B and C reduced to 0.91, 0.89 and 0.99, respectively. In early stage, the pH value of group C was higher than that of group A and equal to group B, which may be due to the activity of microorganisms being inhibited under higher temperature and DTR conditions, resulting in slow mineral dissolution and a lower rate of acid release. In the middle stage, the pH of group C showed the slowest drop, indicating that the adverse effect of DTR condition significantly increased. However, the adverse effect of DTR condition gradually decreased until it almost disappeared on pH observed in the late stage.

$$2FeS_2 + 2H_2O + 7O_2 \xrightarrow{\text{Bacteria}} 2Fe^{2+} + 4SO_4^{2-} + 4H^+ \qquad (2)$$

Based on these results, it can be concluded that in the early stage, subjection to a DTR or higher temperature conditions may inhibited mineral bio-oxidation, resulting in the formation of less acid and metal ions. In the middle stage, the mineral dissolution rate obviously slow down in the DTR bioleaching group and the DTR inhibition significantly increase. Finally, DTR condition had little effect on the bioleaching results in the late stage.

3.2. Effect of DTR on EPS during bioleaching

Based on the physicochemical properties of the leachate, subjection to a DTR was found to have different degrees of influence on each stage of the bioleaching process. EPS protects bacteria from extreme environmental conditions and is closely related to the interaction between bacteria and minerals (Hu et al., 2020; Li and Sand, 2017). Therefore, in order to further establish the effect of DTR on the bioleaching process, the variation in EPS characteristics of groups A, B and C were assessed at different bioleaching times. Fig. 3 shows the 3D fluorescence spectra of LB-EPS and TB-EPS extracted at different time-points from the bioleaching pulp from group A, B and C, respectively. According to previously published literature (Chen et al., 2003; Ye et al., 2021), the 3D fluorescence spectra can be divided into five regions. Regions I, II and III show humic acid-like substances, while regions IV and V show protein-like substances, with further details provided in Table S3 (Supplementary information).

Results show that the formation of EPS was greatly affected by subjection to a DTR, with the generation of EPS being closely related to the reaction temperature in the bioleaching system (Fig. 3). As the bioleaching process proceeded, the total EPS in group A, B and C exhibited a similar trend of increasing initially and then significantly decreasing (Aguirre et al., 2018; Ye et al., 2021). However, the fluorescence intensity of group A EPS samples reached a maximum level on the 12th day, while those from group C reached a maximum level on the 18th day (Fig. 3). These results are consistent with the variation in physicochemical parameters observed during the bioleaching process (Fig. 2). In the first 12 days, group A microorganisms secreted a large amount of EPS, rapidly reaching the EPS concentration required to protect them from the extremely harsh conditions, resulting in mineral dissolution in group A occurring most rapidly. However, group C exhibited the lowest level of early and meddle EPS production, with subjection to a DTR having an inhibitory effect on microbial EPS release in the early and meddle stage of treatment, indicating that a DTR is not conducive to microbial community adaptation to extreme conditions, resulting in the lowest mineral dissolution rate. However, on the 18th day of treatment, the fluorescence intensity of group C reached a maximum level, eventually providing a good leaching environment for the microbial community, achieving the further dissolution of minerals in group C. Therefore, all three groups achieved similar bioleaching effects at the end of the treatment period. In the early stage of bioleaching, protein-like substances are the main components of EPS, which play a critical role in the construction and mechanical stability of biofilms (Flemming and Wingender, 2010). However, with progression of the bioleaching reaction, the content of humic acid-like substances gradually increased due to bacterial apoptosis and organic matter degradation, which was consistent with the results of previous studies (Li and Sand, 2017). Meanwhile, the fluorescence intensity of the LB-EPS layer was more intense than that of the TB-EPS layer at the same bioleaching time, indicating that most of the total EPS was enriched in the LB-EPS layer. It is of note, that although EPS formation by group A, B and C microbes changed greatly with varying reaction temperature conditions, subjection to a DTR did not alter the composition or three-dimensional structure of the EPS matrix. This may a relevant factor in the recovery of the minerals dissolution effect by group C, which gradually increased and achieved the same level of mineral dissolution as group A and group B in the late stage. Previous studies have not systematically analyzed the relationship between subjection to a DTR and EPS formation (Li and Sand, 2017; Yu et al., 2018); therefore, these findings provide a more comprehensive understanding of the effect of DTR conditions on microbial responses during the bioleaching process.

Humic acid is a commonly occurring dissolved organic compound in nature and its role in the bioleaching process has been well established (Hu et al., 2020; Zhang et al., 2020). In order to quantify the fluorescent signal of humic acid-like substances in the 3D fluorescence spectra (Fig. 3), the FRI of humic acid-like substances was calculated and the results are provided in Table S4 (Supplementary information). It can be seen from Table S3 and Fig. 4a that the trend of change in humic acid-like substances in EPS samples was similar for all three bioleaching groups, exhibiting an initially gradual increase and then a significant decreasing trend. However, the concentration level of humic acid-like substances in EPS in each treatment group was significantly different at the same treatment time. On the 12th day of bioleaching, the concentrations of humic acid-like substances in the EPS of groups A, B and C were 147.10×10^4 RU, 51.34×10^4 RU and 30.94×10^4 RU, respectively. Obviously, the concentration of protein-like substances of group C was significantly lower than that of group A and B. These results follow a similar trend to the changes in physicochemical parameters during bioleaching (Fig. 2). Humic acid-like substances are formed during bacterial degradation and gradually accumulate throughout the bioleaching process. In the late stage of bioleaching, the concentration of humic acid-like substances decreased gradually in all treatment groups, which may be due to the low metabolic ability of bacteria or the increase in acid stress causing cell membrane abscission (Feng et al., 2015; Zhang et al., 2019). High levels of humic acid production can improve the resistance of cells to heat denaturation, proteolysis and dehydration (Flemming et al., 2016). In addition, amino, carboxyl, phenol, and sulfhydryl functional groups in humic acids can be used as potential binding sites for toxic metal ions (Rashid et al., 2018; Zhang et al., 2020), reducing the toxicity induced by high concentrations of metal ions. In the early and middle stages of treatment, subjection to a DTR was not conducive to the formation humic acid-like substances, resulting in lower bioleaching efficiency. By the 18th day of treatment, there was a rapid increase in the formation of humic acid-like substances in group C, providing protection against extreme environmental conditions and increasing the rate of mineral dissolution and finally, all three bioleaching groups achieved similar bioleaching effects. Meanwhile, polyaromatic-type humic acid II was found to exhibit the most obvious change in humic acid-like substance concentrations, indicating that these substances may contribute significantly to the bioleaching process.

Extracellular proteins are important components of EPS matrix, which are closely related to maintaining the mechanical stability of cells and determining the structure of biofilms (Flemming and Wingender, 2010; Li and Sand, 2017). It can be seen that, as a function of bioleaching time, the generation behavior of protein-like substances was relatively different between different treatment conditions (Fig. 4b). Similar phenomena had been found in previous studies (Chu et al., 2021). These results might be due to a combination of protein secretion and degradation during bioleaching (Flemming and Wingender, 2010). In addition, on the 12th day of bioleaching, the FRI values of protein-like substances in the EPS of group A, B and C were 113.70×10^4 RU, 85.53×10^4 RU and 64.06×10^4 RU, respectively. It can be clearly observed that the group C FRI value of protein-like substances was significantly lower than that of group A and B, indicating that subjection to a DTR significantly inhibited the secretion of protein-like substances by microbes in the early and middle stages. It is generally believed that the increase of protein content is beneficial to bioleaching process (Yu et al., 2019; Zhang et al., 2019). The lack of protein in the initial stage of DTR group resulted in its low mineral dissolution efficiency. However, by the 18th day, the protein-like substances of group C exhibited a sharp increase, leading to the rapid dissolution of minerals (Fig. 2).

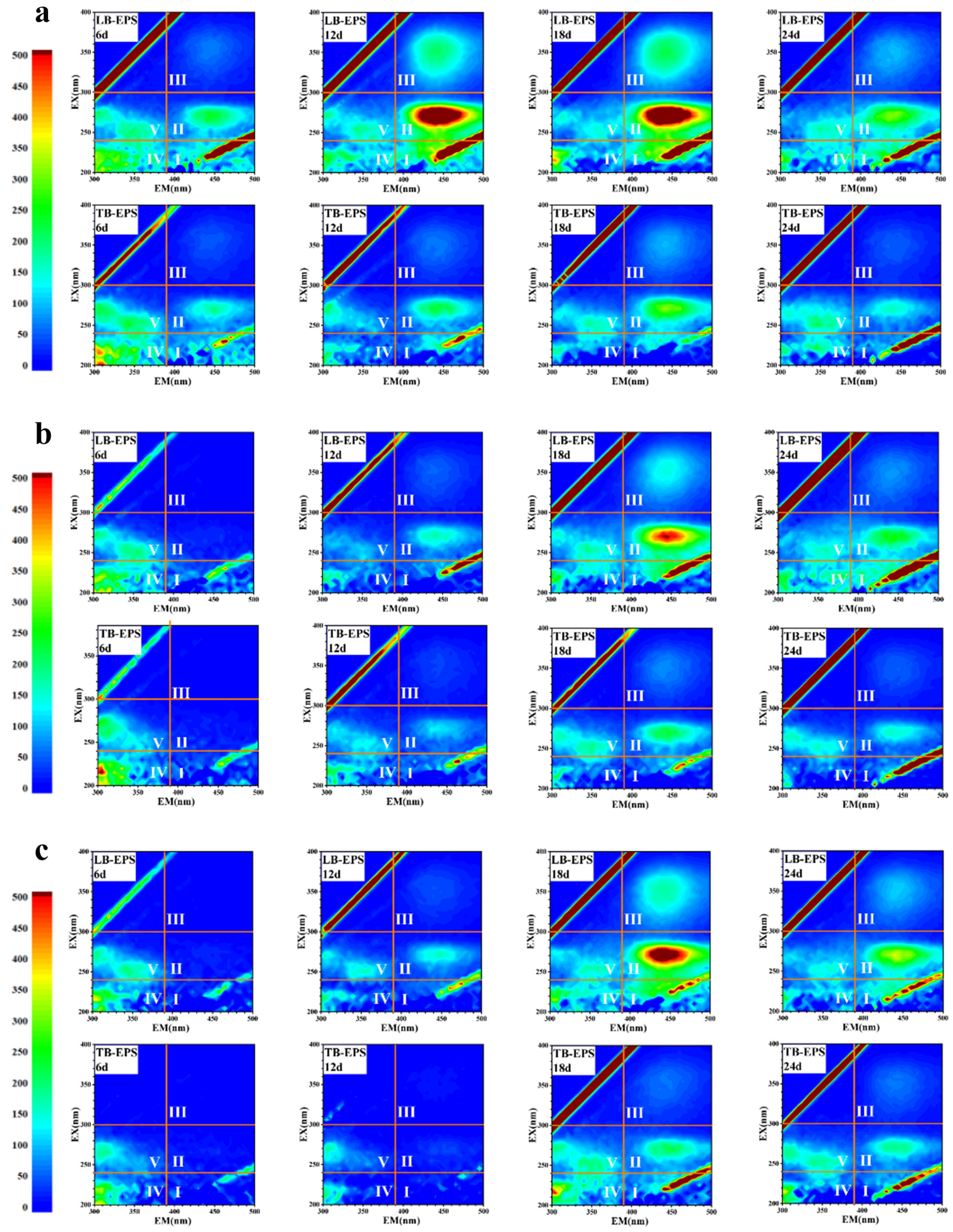

Fig. 3. The 3D-EEM fluorescence images of EPS (LB-EPS, TB-EPS) in different bioleaching treatment groups: (a) group A; (b) group B; (c) group C.

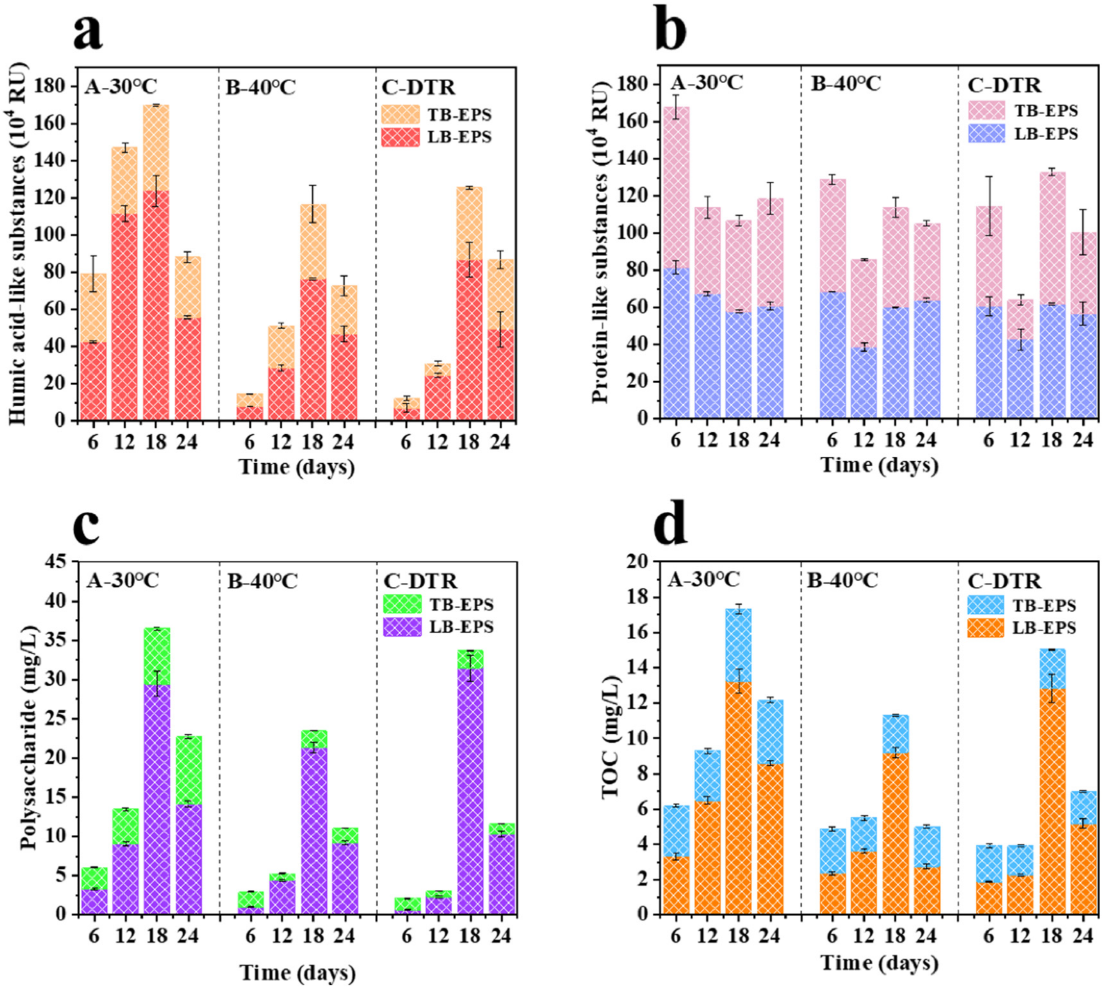

Fig. 4. The variation in organic matter concentrations in different EPS fractions: loosely bound EPS (LB-EPS) and tightly bound EPS (TB-EPS) during the bioleaching treatment process. (a) Humic acid-like substances; (b) protein-like substances; (c) polysaccharides; (d) TOC. In each sub-figure, the results for groups A (30 °C), B (40 °C), and C (DTR) are presented.

With the progression of bioleaching, the polysaccharides in EPS samples from all three groups also exhibited an initial gradually increasing trend, followed by a rapid decrease, with all three treatment groups reaching maximum values on the 18th day (Fig. 4c). However, significant differences were observed in the polysaccharide concentrations produced under different treatment conditions. On the 12th day, the EPS polysaccharide concentrations of group A, B and C were 13.49 mg/L, 5.26 mg/L and 3.03 mg/L, respectively. By the 18th day, the polysaccharide concentration of group C exhibited a sharp increase, leading to the rapid dissolution of minerals. These results indicate that although DTR conditions were not conducive to the secretion of polysaccharides by microbial communities in the early and meddle stage of treatment, the continuous production of polysaccharides resulted in a gradual decrease in the effect of DTR inhibition on microbial communities and finally, all three bioleaching groups achieved a similar bioleaching efficiency. It can be seen that the pattern of change in polysaccharide levels followed a similar trend to the changes in physicochemical properties observed in the leachate (Fig. 2). Polysaccharides are associated with the interaction and attachment of bacteria to mineral surfaces (Mitsunobu et al., 2016; Zhang et al., 2019). Therefore, an increase in polysaccharide content is beneficial for bacterial adherence to mineral surfaces, promoting mineral dissolution. Anionic functional groups from polysaccharides, such as carboxyl groups, can combine with Fe^{3+}, resulting in the formation of Fe^{3+}-EPS complexes on mineral surfaces (La Vars et al., 2018; Muravyov and Panyushkina, 2020). A large amount of Fe^{3+} accumulation between the mineral surface and EPS matrix, increases the rate of oxidative attack and therefore, enhances mineral dissolution (Huang et al., 2019).

TOC is used to express the total amount of organic matter such as proteins, humic acids and polysaccharides in the bioleaching solution (Zhao et al., 2019). Therefore, a change in TOC content can reflect changes in the total EPS content during the bioleaching process, to a certain extent. As shown in Fig. 4d, the TOC content increased continuously in all bioleaching groups, reaching maximum levels by the 18th day of treatment, indicating that EPS secreted by bacteria increased rapidly at this period. In contrast, during the late stage of bioleaching (from 18 to 24 days), the TOC content decreased significantly, which may be due to the continual deterioration in the environment leading to detachment of the biofilm from mineral surfaces (Feng et al., 2015). On the 12th day of bioleaching, the TOC concentrations of group A, B and C were 9.31 mg/L, 5.50 mg/L and 3.91 mg/L, respectively. It can be clearly observed that the group C TOC concentration was significantly lower than that of group A and B, indicating that subjection to a DTR significantly inhibited the secretion of EPS by microbes in the early and middle stages. However, by the 18th day, the TOC concentration of group C exhibited a sharp increase, leading to the rapid dissolution of minerals (Fig. 2a). These results indicate that the continuous production of EPS provided protection for microbial communities in extreme environments, resulting in a gradual decrease in the effect of DTR inhibition on microbial communities, and finally, all three bioleaching groups achieved a similar bioleaching efficiency.

In addition, most organics were mainly enriched in LB-EPS layer under different treatment conditions (Fig. 4). LB-EPS is diffused from TB-EPS surrounding the cell (Li and Yang, 2007). It has been reported that LB-EPS can enhance the aggregation process of cells and improve the adhesion to sediment particles through greater hydrophobic interaction (Zhao et al., 2015). Meanwhile, the adsorption capacity of LB-EPS for heavy metal ions is higher than that of TB-EPS (Y. Li et al., 2021; Sun et al., 2009). In this study, the content of LB-EPS was higher than that of TB-EPS (Fig. 4). Y. Li et al. (2021) reported similar results in the study on EPS yield of *Enterobacter* sp. FM-1 (FM-1). Therefore, it was speculated that in the bioleaching of metal sulfide ore, the higher content of LB-EPS was conducive to the bacteria adhesion on the mineral surface and enhanced the adsorption capacity of metal ions, which promoted the mineral dissolution.

Based on these results, it can be concluded that subjection to a DTR did not change the composition of the microbial EPS matrix (humic acid-like substances, polysaccharides and protein-like substances). In contrast, DTR conditions had a major effect on the production of EPS in the bioleaching process, initially inhibiting EPS secretion and reducing the rate of mineral bio-oxidation. However, continual EPS production in the bioleaching system gradually increased EPS concentrations, reducing the adverse effects of DTR conditions on mineral dissolution.

3.3. Effect of DTR conditions on the mineralography of sulfide ore

To establish whether DTR conditions affect mineral bio-oxidation, the mineralogphy of sulfide ore were studied by XRD, FTIR and SEM-EDS.

3.3.1. Mineralogical phase analysis

XRD patterns showed that the leaching residues were mainly composed of gypsum, calcite and pyrite (Fig. 5). Compared with the original mineral material (Fig. 1), the pyrite peak in the material subjected to the abiotic treatment was not obviously weakened, indicating that the effect of acid leaching on mineral dissolution was negligible. In contrast, compared with the abiotic group, the pyrite peaks in the XRD spectra for bioleaching treatment groups were obviously reduced, indicating that pyrite in HPSO was greatly oxidized and destroyed by the microbial community during the bioleaching process, resulting in the release of iron ions. However, there was no obvious difference in the phase composition of the final bioleaching residues of groups A, B and C, indicating that subjection to DTR condition had little impact on the final bioleaching results. According to previous reports, the dissolution of pyrite leads to the formation of a large amount of jarosite, which inhibits the further dissolution of minerals (Yang et al., 2020). Interestingly, jarosite was not detected in the bioleaching residues from all three treatment groups, which may be due to the low pH conditions of the

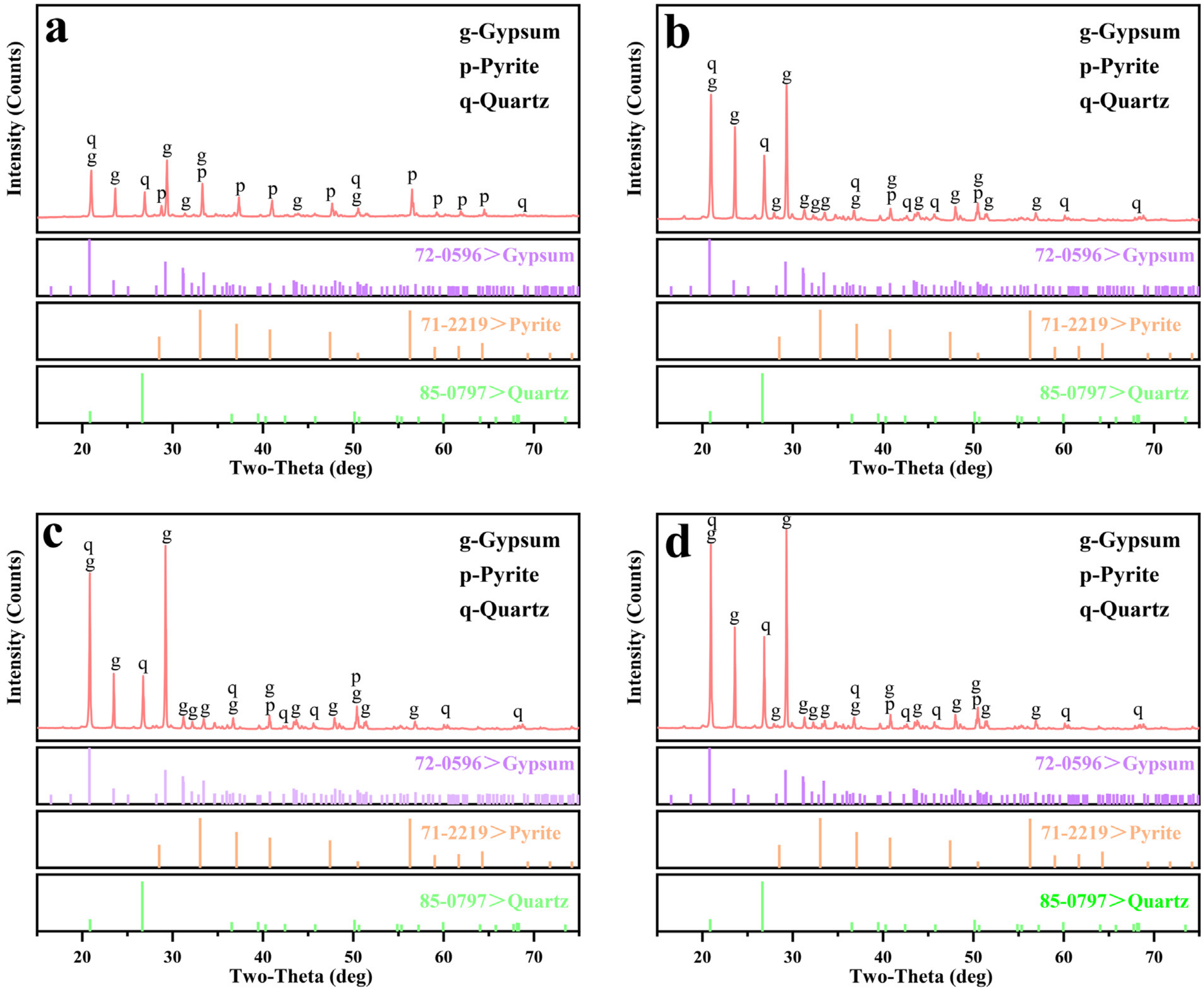

Fig. 5. XRD spectra of the acid leaching residue from the (a) abiotic control group treated at 30 °C; (b) group A bioleaching treatment at 30 °C; (c) group B bioleaching treatment at 40 °C; (d) group C bioleaching treatment under DTR.

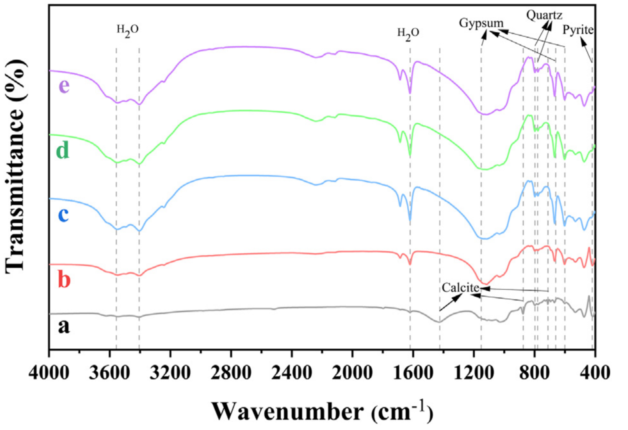

Fig. 6. FTIR spectrograms of (a) the original HPSO mineral; (b) the acid leaching residue from the abiotic control experiment at 30 °C; (c) the bioleaching residue from group A at 30 °C; (d) the bioleaching residue from group B at 40 °C; (e) the bioleaching residue from group C under DTR.

bioleaching system (Fig. 2d), preventing the formation of jarosite (Chen et al., 2015). The results of XRD analysis showed that DTR did not affect the mineral dissolution mechanism, with low pH conditions inhibiting the formation of jarosite, supporting the continual bacterial oxidization of minerals.

3.3.2. FTIR analysis of sulfide ore

In order to better understand the mechanism of metal dissolution, FTIR was used to systematically study the composition change of acid treated ores and to establish the process of ore configuration change by the acidophilic bacterial communities under different reaction temperature conditions. The FTIR spectrogram results shown in Fig. 6 were basically consistent with the XRD spectrograms shown in Fig. 5. The peaks at 1425, 875 and 712 cm^{-1} represent calcite and were only observed in the original mineral (Li et al., 2020; Shirsath et al., 2016), as calcite rapidly reacts with hydrogen ions and dissolves in the leaching system. The peak in the range of 798–779 cm^{-1} was mainly attributed to Si-O-Si inter-tetrahedral bridging bonds in quartz (Partyka et al., 2014), while the peaks at 3556, 3406, 1620, 1152, 661, and 601 cm^{-1} were attributed to gypsum and its crystal water (Ashfaq et al., 2020; Ennaciri et al., 2019; Ma et al., 2020). Stronger and sharper characteristic gypsum peaks were observed in the FTIR spectrograms of bioleaching residues, indicating that bacteria promoted sulfur oxidation and produced more sulfate ions for the formation of gypsum. The peak at 420 cm^{-1} was attributed to the presence of pyrite in leaching residues (Tang et al., 2021). Compared with the original HPSO mineral material, the peak at 420 cm^{-1} was only slightly weakened in the acid leaching residue, indicating that acid leaching alone had a minor effect on pyrite. However, the peak at 420 cm^{-1} almost completely disappeared in the bioleaching residue, indicating that most pyrite in HPSO was bio-oxidized and dissolved. The residues of all three bioleaching groups exhibited similar peak changes, reflecting that DTR condition did not alter the final mechanism of mineral dissolution.

3.3.3. Microstructure and elemental composition of sulfide ore

SEM was used to assess the surface morphology of the original HPSO mineral, acid leaching residues and bioleaching residues (Fig. 7). Results show that the original HPSO mineral surface was clean and smooth, with only a few surface bound particles (Fig. 7a). In the abiotic control systems, the surface of the treated mineral remained smooth and dense, with some debris present on the surface (Fig. 7b), indicating

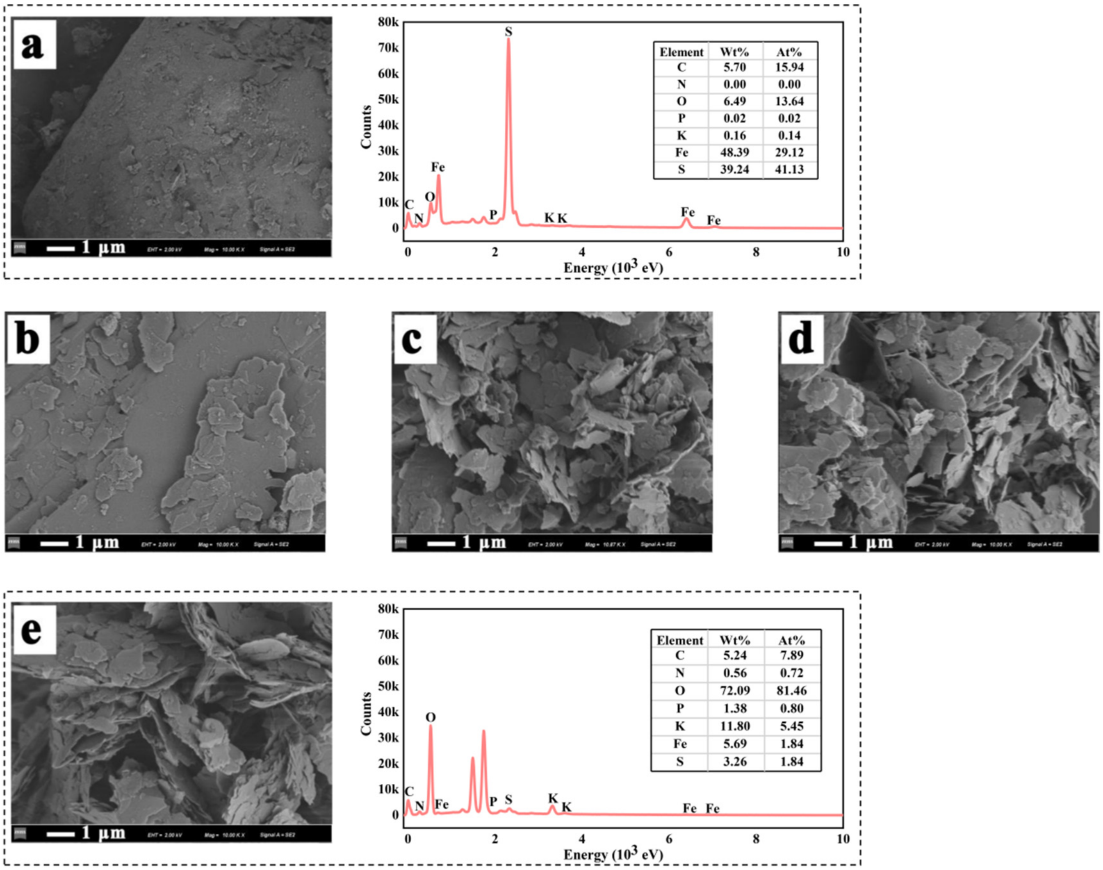

Element	Wt%	At%
C	5.70	15.94
N	0.00	0.00
O	6.49	13.64
P	0.02	0.02
K	0.16	0.14
Fe	48.39	29.12
S	39.24	41.13

Element	Wt%	At%
C	5.24	7.89
N	0.56	0.72
O	72.09	81.46
P	1.38	0.80
K	11.80	5.45
Fe	5.69	1.84
S	3.26	1.84

Fig. 7. SEM-EDS images of the (a) original mineral; (b) acid leaching residue from the abiotic control experiment at 30 °C; (c) bioleaching residue from group B at 40 °C; (d) bioleaching residue from group C under DTR; (e) bioleaching residue from group A at 30 °C.

that acid leaching had a weak capacity for mineral degradation. After treatment with the microbial community, the mineral surfaces changed obviously, with a large number of loose sheet structures observed, indicating that the mineral was degraded and dissolved significantly under the action of bacteria. A large number of loose gaps on the bioleaching residue surface could be used as microbial adsorption sites, which is conducive to the complete utilization of minerals by bacteria (Huang et al., 2019). In addition, the surface of bioleaching residues was covered by bioleaching products, verifying that the bacterial treatment changed the surface morphology of minerals (Fig. 7c–e). Interestingly, there were no significant differences observed in the surface corrosion of bioleaching residues from group A, B and C, indicating that the variation in culture temperature had little effect on the final bioleaching results. In order to determine the composition of the products bound to the mineral surface, EDS was performed on the original HPSO mineral and group A bioleaching residue to establish the proportions of elements on the mineral surfaces. Compared with the original HPSO mineral, the concentration of Fe in the group A residue was greatly reduced, indicating that bacteria can effectively promote the dissolution of pyrite from HPSO, which is in agreement with the bioleaching (Fig. 2) and XRD (Fig. 5) results. In addition, N, O, K, and P increased significantly on the mineral surface after bioleaching. These elements are typical biological elements and therefore, it may be speculated that biofilms or EPS may adhere to the mineral surface (Liu et al., 2020; Zeng et al., 2020), promoting mineral dissolution. The results of SEM-EDS analysis show that EPS secreted by bacteria adhere to the mineral surface, facilitating the effective bioleaching of minerals, with subjection to a DTR having little effect on the final bioleaching result.

3.4. Potential value for industrial application

This study investigated the effect of DTR on bioleaching of sulfide ore by an artificial microbial consortium. The result showed that EPS was closely related to bioleaching efficiency, which was consistent with previous study (Hu et al., 2020; Li and Sand, 2017). However, DTR induced inhibition of the EPS secretion, leading to low bioleaching efficiency in the early and middle stages. In addition, DTR had no obvious effect on the mineralogical characteristics of sulfide ore. Temperature is a key factor affecting bioleaching efficiency (Boxall et al., 2017; Yu et al., 2019), and DTR is a practical aspect that will be encountered in the industrial application of bioleaching by artificial microbial community (J.F. Li et al., 2021). However, few studies investigated the effect of DTR on bioleaching. Therefore, this study helps to improve our understanding of the effect of DTR on bioleaching and has important guiding significance for promoting artificial microbial community from laboratory level studies to industrial application. For effective industrial application, in order to accelerate the start-up process of artificial microbial community treatment systems, enhanced temperature control measures were recommended in the bioleaching process to reduce the adverse effects of DTR conditions.

4. Conclusions

This is the first study of the effect of DTR conditions on bioleaching of sulfide ore. The main conclusions are as follows:

(1) DTR had an obviously inhibitory effect on the sulfide ore bioleaching efficiency of an artificial microbial community, but this effect was mainly concentrated in the early and middle stages of treatment (0–18 days), gradually decreasing until almost disappearing in the late stage (18–24 days).
(2) DTR inhibited the production of microbial EPS in the early and middle stages of treatment, with the continuous increase in EPS in the bioleaching system being beneficial for reducing the inhibition of DTR conditions on mineral dissolution.
(3) The results of XRD, FTIR and SEM analysis confirmed that the DTR had no obvious effect on the mineralography of sulfide ore.
(4) For effective industrial application, in order to accelerate the start-up process of artificial microbial community treatment systems, temperature control measures should be increased in the bioleaching process to reduce the adverse effects of DTR conditions.

CRediT authorship contribution statement

Xiaodi Fang: Methodology, Formal analysis, Data curation, Writing – original draft, Writing – review & editing. **Shuiyu Sun:** Conceptualization, Validation, Supervision, Project administration. **Xiaojian Liao:** Methodology, Formal analysis, Writing – review & editing. **Shoupeng Li:** Conceptualization, Formal analysis, Supervision, Writing – review & editing. **Siyu Zhou:** Methodology, Formal analysis, Supervision. **Qiaowei Gan:** Methodology, Investigation. **Liuting Zeng:** Methodology, Investigation. **Zhijie Guan:** Methodology, Formal analysis.

Declaration of competing interest

The authors declare that they have no known competing financial interests or personal relationships that could have appeared to influence the work reported in this paper.

Acknowledgments

The authors greatly acknowledge the financial support from the National Key Research and Development Program of China (No. 2018YFD0800700) and Application Research Project from Department of Education of Guangdong Province (2017GKZDXM007).

Appendix A. Supplementary data

Supplementary data to this article can be found online at https://doi.org/10.1016/j.scitotenv.2021.150234.

References

Aguirre, P., Guerrero, K., Sanchez-Rodriguez, A., Gentina, J.C., Schippers, A., 2018. Making sticky cells: effect of galactose and ferrous iron on the attachment of leptospirillum ferrooxidans to mineral surfaces. Res. Microbiol. 169, 569–575. https://doi.org/10.1016/j.resmic.2018.08.005.

Ashfaq, M.Y., Al-Ghouti, M.A., Da'na, D.A., Qiblawey, H., Zouari, N., 2020. Effect of concentration of calcium and sulfate ions on gypsum scaling of reverse osmosis membrane, mechanistic study. J. Mater. Res. Technol. 9, 13459–13473. https://doi.org/10.1016/j.jmrt.2020.09.117.

Banerjee, I., Burrell, B., Reed, C., West, A.C., Banta, S., 2017. Metals and minerals as a biotechnology feedstock: engineering biomining microbiology for bioenergy applications. Curr. Opin. Biotechnol. 45, 144–155. https://doi.org/10.1016/j.copbio.2017.03.009.

Bellenberg, S., Huynh, D., Poetsch, A., Sand, W., Vera, M., 2019. Proteomics reveal enhanced oxidative stress responses and metabolic adaptation in acidithiobacillus ferrooxidans biofilm cells on pyrite. Front. Microbiol. 10, 592. https://doi.org/10.3389/fmicb.2019.00592.

Blight, K., Ralph, D.E., Thurgate, S., 2000. Pyrite surfaces after bio-leaching: a mechanism for bio-oxidation. Hydrometallurgy 58, 227–237. https://doi.org/10.1016/S0304-386X(00)00136-5.

Boxall, N.J., Rea, S.M., Li, J., Morris, C., Kaksonen, A.H., 2017. Effect of high sulfate concentrations on chalcopyrite bioleaching and molecular characterisation of the bioleaching microbial community. Hydrometallurgy 168, 32–39. https://doi.org/10.1016/j.hydromet.2016.07.006.

Brierley, J.A., 2008. A perspective on developments in biohydrometallurgy. Hydrometallurgy 94, 2–7. https://doi.org/10.1016/j.hydromet.2008.05.014.

Brierley, J.A., Brierley, C.L., 2001. Present and future commercial applications of biohydrometallurgy. Hydrometallurgy 59, 233–239. https://doi.org/10.1016/S0304-386X(00)00162-6.

Camacho, D., Frazao, R., Fouillen, A., Nanci, A., Lang, B.F., Apte, S.C., et al., 2020. New insights into acidithiobacillus thiooxidans sulfur metabolism through coupled gene expression, solution chemistry, microscopy, and spectroscopy analyses. Front. Microbiol. 11, 411. https://doi.org/10.3389/fmicb.2020.00411.

Chen, W., Westerhoff, P., Leenheer, J.A., Booksh, K., 2003. Fluorescence excitation - emission matrix regional integration to quantify spectra for dissolved organic matter. Environ. Sci. Technol. 37, 5701–5710. https://doi.org/10.1021/es034354c.

Chen, S., Yang, Y.K., Liu, C.Q., Dong, F.Q., Liu, B.J., 2015. Column bioleaching copper and its kinetics of waste printed circuit boards (WPCBs) by acidithiobacillus ferrooxidans. Chemosphere 141, 162–168. https://doi.org/10.1016/j.chemosphere.2015.06.082.

Chu, H., Wang, J., Tian, B., Qian, C., Niu, T., Qi, S., et al., 2021. Generation behavior of extracellular polymeric substances and its correlation with extraction efficiency of valuable metals and change of process parameters during bioleaching of spent petroleum catalyst. Chemosphere 275, 130006. https://doi.org/10.1016/j.chemosphere.2021.130006.

Ennaciri, Y., El Alaoui-Belghiti, H., Bettach, M., 2019. Comparative study of K2SO4 production by wet conversion from phosphogypsum and synthetic gypsum. J. Mater. Res. Technol. 8, 2586–2596. https://doi.org/10.1016/j.jmrt.2019.02.013.

Feng, S., Yang, H., Wang, W., 2015. System-level understanding of the potential acid-tolerance components of acidithiobacillus thiooxidans ZJJN-3 under extreme acid stress. Extremophiles 19, 1029–1039. https://doi.org/10.1007/s00792-015-0780-z.

Flemming, H.C., Wingender, J., 2010. The biofilm matrix. Nat. Rev. Microbiol. 8, 623–633. https://doi.org/10.1038/nrmicro2415.

Flemming, H.C., Wingender, J., Szewzyk, U., Steinberg, P., Rice, S.A., Kjelleberg, S., 2016. Biofilms: an emergent form of bacterial life. Nat. Rev. Microbiol. 14, 563–575. https://doi.org/10.1038/nrmicro.2016.94.

Hu, W., Feng, S., Tong, Y., Zhang, H., Yang, H., 2020. Adaptive defensive mechanism of bioleaching microorganisms under extremely environmental acid stress: advances and perspectives. Biotechnol. Adv. 42, 107580. https://doi.org/10.1016/j.biotechadv.2020.107580.

Huang, Z., Feng, S., Tong, Y., Yang, H., 2019. Enhanced "contact mechanism" for interaction of extracellular polymeric substances with low-grade copper-bearing sulfide ore in bioleaching by moderately thermophilic acidithiobacillus caldus. J. Environ. Manag. 242, 11–21. https://doi.org/10.1016/j.jenvman.2019.04.030.

Igarashi, T., Herrera, P.S., Uchiyama, H., Miyamae, H., Iyatomi, N., Hashimoto, K., et al., 2020. The two-step neutralization ferrite-formation process for sustainable acid mine drainage treatment: removal of copper, zinc and arsenic, and the influence of coexisting ions on ferritization. Sci. Total Environ. 715, 136877. https://doi.org/10.1016/j.scitotenv.2020.136877.

Jia, Y., Sun, H.-y., Tan, Q.-y., Gao, H.-s., Feng, X.-l., Ruan, R.-m., 2018. Linking leach chemistry and microbiology of low-grade copper ore bioleaching at different temperatures. Int. J. Miner. Metall. Mater. 25, 271–279. https://doi.org/10.1007/s12613-018-1570-2.

Karamanev, D.G., Nikolov, L.N., Mamatarkova, V., 2002. Rapid simultaneous quantitative determination of ferric and ferrous ions in drainage waters and similar solutions. Miner. Eng. 15, 341–346. https://doi.org/10.1016/S0892-6875(02)00026-2.

La Vars, S., Newton, K., Quinton, J., Cheng, P.-Y., Wei, D.-H., Chan, Y.-L., et al., 2018. Surface chemical characterisation of pyrite exposed to acidithiobacillus ferrooxidans and associated extracellular polymeric substances. Minerals 8, 132. https://doi.org/10.3390/min8040132.

Li, Q., Sand, W., 2017. Mechanical and chemical studies on EPS from sulfobacillus thermosulfidooxidans: from planktonic to biofilm cells. Colloids Surf. B: Biointerfaces 153, 34–40. https://doi.org/10.1016/j.colsurfb.2017.02.009.

Li, X.Y., Yang, S.F., 2007. Influence of loosely bound extracellular polymeric substances (EPS) on the flocculation, sedimentation and dewaterability of activated sludge. Water Res. 41, 1022–1030. https://doi.org/10.1016/j.watres.2006.06.037.

Li, Y., Kawashima, N., Li, J., Chandra, A.P., Gerson, A.R., 2013. A review of the structure, and fundamental mechanisms and kinetics of the leaching of chalcopyrite. Adv. Colloid Interf. Sci. 197, 1–32. https://doi.org/10.1016/j.cis.2013.03.004.

Li, L., Yang, Y., Lv, Y.R., Yin, P., Lei, T., 2020. Porous calcite CaCO3 microspheres: preparation, characterization and release behavior as doxorubicin carrier. Colloids Surf. B: Biointerfaces 186, 110720. https://doi.org/10.1016/j.colsurfb.2019.110720.

Li, J.F., Yang, H.Y., Tong, L.L., Sand, W., 2021a. Some aspects of industrial heap bioleaching technology: from basics to practice. Miner. Process. Extr. Metall. Rev. https://doi.org/10.1080/08827508.2021.1893720.

Li, Y., Xin, M., Xie, D., Fan, S., Ma, J., Liu, K., et al., 2021b. Variation in extracellular polymeric substances from enterobacter sp. and their Pb2+ adsorption behaviors. ACS Omega 6, 9617–9628. https://doi.org/10.1021/acsomega.1c00185.

Liang, J., Huang, J., Zhang, S., Yang, X., Huang, S., Zheng, L., et al., 2019. A highly efficient conditioning process to improve sludge dewaterability by combining calcium hypochlorite oxidation, ferric coagulant re-flocculation, and walnut shell skeleton construction. Chem. Eng. J. 361, 1462–1478. https://doi.org/10.1016/j.cej.2018.10.143.

Liao, X., Sun, S., Zhou, S., Ye, M., Liang, J., Huang, J., et al., 2019. A new strategy on biomining of low grade base-metal sulfide tailings. Bioresour. Technol. 294, 122187. https://doi.org/10.1016/j.biortech.2019.122187.

Liu, S., Hong, M., Wang, X., Yang, B., Lin, H., Lin, M., et al., 2020. Pretreatment with acidic ferric sulfate leaching promotes the bioleaching of bornite. Hydrometallurgy 196, 105349. https://doi.org/10.1016/j.biortech.2019.122187.

Ma, L., Wang, H., Wu, J., Wang, Y., Zhang, D., Liu, X., 2019. Metatranscriptomics reveals microbial adaptation and resistance to extreme environment coupling with bioleaching performance. Bioresour. Technol. 280, 9–17. https://doi.org/10.1016/j.biortech.2019.01.117.

Ma, X., Yao, S.H., Yuan, Z.D., Bi, R., Wu, X., Zhang, J.X., et al., 2020. Detoxification and reclamation of hydrometallurgical arsenic- and trace metals-bearing gypsum via hydrothermal recrystallization in acid solution. Chemosphere 250, 126290. https://doi.org/10.1016/j.chemosphere.2020.126290.

Mitsunobu, S., Zhu, M., Takeichi, Y., Ohigashi, T., Suga, H., Jinno, M., et al., 2016. Direct detection of Fe(II) in extracellular polymeric substances (EPS) at the mineral-microbe Interface in bacterial pyrite leaching. Microbes Environ. 31, 63–69. https://doi.org/10.1264/jsme2.ME15137.

More, T.T., Yadav, J.S., Yan, S., Tyagi, R.D., Surampalli, R.Y., 2014. Extracellular polymeric substances of bacteria and their potential environmental applications. J. Environ. Manag. 144, 1–25. https://doi.org/10.1016/j.jenvman.2014.05.010.

Muravyov, M., Panyushkina, A., 2020. Distinct roles of acidophiles in complete oxidation of high-sulfur ferric leach product of zinc sulfide concentrate. Microorganisms 8, 386. https://doi.org/10.3390/microorganisms8030386.

Panda, S., Akcil, A., Pradhan, N., Deveci, H., 2015. Current scenario of chalcopyrite bioleaching: a review on the recent advances to its heap-leach technology. Bioresour. Technol. 196, 694–706. https://doi.org/10.1016/j.biortech.2015.08.064.

Partyka, J., Gajek, M., Gasek, K., 2014. Effects of quartz grain size distribution on the structure of porcelain glaze. Ceram. Int. 40, 12045–12053. https://doi.org/10.1016/j.ceramint.2014.04.044.

Premnath, N., Mohanrasu, K., Guru Raj Rao, R., Dinesh, G.H., Siva Prakash, G., Pugazhendhi, A., et al., 2021. Effect of C/N substrates for enhanced extracellular polymeric substances (EPS) production and poly cyclic aromatic hydrocarbons (PAHs) degradation. Environ. Pollut. 275, 116035. https://doi.org/10.1016/j.envpol.2020.116035.

Rashid, M., Sterbinsky, G.E., Pinilla, M.A.G., Cai, Y., O'Shea, K.E., 2018. Kinetic and mechanistic evaluation of inorganic arsenic species adsorption onto humic acid grafted magnetite nanoparticles. J. Phys. Chem. C 122, 13540–13547. https://doi.org/10.1021/acs.jpcc.7b12438.

Sethurajan, M., van Hullebusch, E.D., Nancharaiah, Y.V., 2018. Biotechnology in the management and resource recovery from metal bearing solid wastes: recent advances. J. Environ. Manag. 211, 138–153. https://doi.org/10.1016/j.jenvman.2018.01.035.

Shirsath, S.R., Bhanvase, B.A., Sonawane, S.H., Gogate, P.R., Pandit, A.B., 2016. A novel approach for continuous synthesis of calcium carbonate using sequential operation of two sonochemical reactors. Ultrason. Sonochem. 35, 124–133. https://doi.org/10.1016/j.ultsonch.2016.09.009.

Sun, X.F., Wang, S.G., Zhang, X.M., Chen, J.P., Li, X.M., Gao, B.Y., et al., 2009. Spectroscopic study of Zn2+ and Co2+ binding to extracellular polymeric substances (EPS) from aerobic granules. J. Colloid Interface Sci. 335, 11–17. https://doi.org/10.1016/j.jcis.2009.03.088.

Tabelin, C.B., Corpuz, R.D., Igarashi, T., Villacorte-Tabelin, M., Alorro, R.D., Yoo, K., et al., 2020. Acid mine drainage formation and arsenic mobility under strongly acidic conditions: importance of soluble phases, iron oxyhydroxides/oxides and nature of oxidation layer on pyrite. J. Hazard. Mater. 399, 122844. https://doi.org/10.1016/j.jhazmat.2020.122844.

Tang, J., Zhao, B., Lyu, H., Li, D., 2021. Development of a novel pyrite/biochar composite (BM-FeS2@BC) by ball milling for aqueous Cr(VI) removal and its mechanisms. J. Hazard. Mater. 413, 125415. https://doi.org/10.1016/j.jhazmat.2021.125415.

Tian, Yu., 2008. Behaviour of bacterial extracellular polymeric substances from activated sludge: a review. Int. J. Environ. Pollut. 32, 78–89. https://doi.org/10.1504/IJEP.2008.016900.

Xia, J.-l., Song, J.-j., Liu, H.-c., Nie, Z.-y., Shen, L., Yuan, P., et al., 2018. Study on catalytic mechanism of silver ions in bioleaching of chalcopyrite by SR-XRD and XANES. Hydrometallurgy 180, 26–35. https://doi.org/10.1016/j.hydromet.2018.07.008.

Yang, Y., Liu, W., Chen, M., 2015. XANES and XRD study of the effect of ferrous and ferric ions on chalcopyrite bioleaching at 30 °C and 48 °C. Miner. Eng. 70, 99–108. https://doi.org/10.1016/j.mineng.2014.08.021.

Yang, B., Lin, M., Fang, J., Zhang, R., Luo, W., Wang, X., et al., 2020. Combined effects of jarosite and visible light on chalcopyrite dissolution mediated by acidithiobacillus ferrooxidans. Sci. Total Environ. 698, 134175. https://doi.org/10.1016/j.scitotenv.2019.134175.

Ye, M., Li, G., Yan, P., Ren, J., Zheng, L., Han, D., et al., 2017. Removal of metals from lead-zinc mine tailings using bioleaching and followed by sulfide precipitation. Chemosphere 185, 1189–1196. https://doi.org/10.1016/j.chemosphere.2017.07.124.

Ye, M., Liang, J., Liao, X., Li, L., Feng, X., Qian, W., et al., 2021. Bioleaching for detoxification of waste flotation tailings: relationship between EPS substances and bioleaching behavior. J. Environ. Manag. 279, 111795. https://doi.org/10.1016/j.jenvman.2020.111795.

Yu, G.H., He, P.J., Shao, L.M., He, P.P., 2008. Stratificationstructure of sludge flocs with implications to dewaterability. Environ. Sci. Technol. 42, 7944–7949. https://doi.org/10.1021/es8016717.

Yu, R., Hou, C., Liu, A., Peng, T., Xia, M., Wu, X., et al., 2018. Extracellular DNA enhances the adsorption of sulfobacillus thermosulfidooxidans strain ST on chalcopyrite surface. Hydrometallurgy 176, 97–103. https://doi.org/10.1016/j.hydromet.2018.01.018.

Yu, R.-l., Liu, Z.-h., Yu, Z.-j., Wu, X.-l., Shen, L., Liu, Y.-d., et al., 2019. Relationship among the secretion of extracellular polymeric substances, heat resistance, and bioleaching ability of metallosphaera sedula. Int. J. Miner. Metall. Mater. 26, 1504–1511. https://doi.org/10.1007/s12613-019-1851-4.

Zeng, W.-m., Peng, Y.-p., Peng, T.-j., Nan, M.-h., Chen, M., Qiu, G.-z., et al., 2020. Electrochemical studies on dissolution and passivation behavior of low temperature bioleaching of chalcopyrite by acidithiobacillus ferrivorans YL15. Miner. Eng. 155, 106416. https://doi.org/10.1016/j.mineng.2020.106416.

Zhang, R., Neu, T.R., Blanchard, V., Vera, M., Sand, W., 2019. Biofilm dynamics and EPS production of a thermoacidophilic bioleaching archaeon. New Biotechnol. 51, 21–30. https://doi.org/10.1016/j.nbt.2019.02.002.

Zhang, D.R., Chen, H.R., Xia, J.L., Nie, Z.Y., Fan, X.L., Liu, H.C., et al., 2020. Humic acid promotes arsenopyrite bio-oxidation and arsenic immobilization. J. Hazard. Mater. 384, 121359. https://doi.org/10.1016/j.jhazmat.2019.121359.

Zhao, W., Yang, S., Huang, Q., Cai, P., 2015. Bacterial cell surface properties: role of loosely bound extracellular polymeric substances (LB-EPS). Colloids Surf. B: Biointerfaces 128, 600–607. https://doi.org/10.1016/j.colsurfb.2015.03.017.

Zhao, J.F., Liu, S.X., Liu, N., Zhang, H., Zhou, Q.Z., Ge, F., 2019. Accelerated productions and physicochemical characterizations of different extracellular polymeric substances from chiorella vulgaris with nano-ZnO. Sci. Total Environ. 658, 582–589. https://doi.org/10.1016/j.scitotenv.2018.12.019.

Zhuang, Y., Zhang, J., 2020. Diurnal asymmetry in future temperature changes over the main belt and road regions. Ecosyst. Health Sustain. 6, 1749530. https://doi.org/10.1080/20964129.2020.1749530.